

# Greenland Ice Sheet surface mass-balance modelling and freshwater flux for 2007, and in a 1995–2007 perspective

Sebastian H. Mernild,<sup>1\*</sup> Glen E. Liston,<sup>2</sup> Christopher A. Hiemstra,<sup>2</sup> Konrad Steffen,<sup>3</sup> Edward Hanna<sup>4</sup> and Jens H. Christensen<sup>5</sup>

<sup>1</sup> International Arctic Research Center and Water & Environmental Research Center, University of Alaska Fairbanks, Alaska, USA

<sup>2</sup> Cooperative Institute for Research in the Atmosphere, Colorado State University, Colorado, USA

<sup>3</sup> Cooperative Institute for Research in Environmental Sciences, University of Colorado, Colorado, USA

<sup>4</sup> Department of Geography, University of Sheffield, UK

<sup>5</sup> Danish Climate Centre, Danish Meteorological Institute, Denmark

## Abstract:

The freshwater flux from the Greenland Ice Sheet (GrIS) to the ocean is of considerable importance to the global eustatic sea level rise. A physical modelling approach using SnowModel, a state-of-the-art snow-evolution modelling system that includes four submodels (MicroMet, EnBal, SnowPack, and SnowTran-3D), was used to quantify the 1995–2007 GrIS surface mass-balance (SMB), including freshwater flux. Meteorological observations from 26 meteorological stations located on the GrIS (Greenland Climate Network; GC-Net stations) and in coastal Greenland (Danish Meteorological Institute (DMI) WMO-stations) were used as model inputs. The GrIS minimum surface melt extent of 29% occurred in 1996, while the greatest extent of 51% was present in 2007. The 2007 melt extent was 20% greater than the average for 1995–2006. The year 2007 had the highest GrIS surface runoff ( $523 \text{ km}^3 \text{ y}^{-1}$ ) and the lowest SMB ( $-3 \text{ km}^3 \text{ y}^{-1}$ ); the only year with a negative GrIS SMB. Runoff in 2007 was approximately 35% greater than average for 1995–2006. From 1995 through 2007 overall, precipitation decreased while ablation increased, leading to an increased average SMB loss of  $127 \text{ km}^3$ . The modelled GrIS SMB was merged with previous estimates of GrIS subglacial runoff (from geothermal melt) and GrIS calving to quantify GrIS freshwater flux to the ocean, indicating an average negative mass-balance of  $265 (\pm 83) \text{ km}^3 \text{ y}^{-1}$ . This study further suggests an average GrIS freshwater flux of approximately  $786 \text{ km}^3 \text{ y}^{-1}$  to the ocean, of which 45% occurs from iceberg calving and geothermal bottom melting. The average annual GrIS freshwater flux equals  $2.1 \pm 0.2 \text{ mm w.eq. y}^{-1}$  in eustatic sea level rise, indicating a cumulative flux of  $28 \text{ mm w.eq.}$  from 1995 through 2007. The average GrIS net loss contributes to a net sea level rise of  $0.7 \pm 0.2 \text{ mm w.eq. y}^{-1}$ , and a cumulative net increase of  $10 \text{ mm w.eq.}$  Copyright © 2009 John Wiley & Sons, Ltd.

KEY WORDS Arctic; Greenland ice sheet; mass loss; runoff; sea level rise; snowmodel; surface mass-balance modeling

Received 8 June 2008; Accepted 5 April 2009

## INTRODUCTION

The Greenland Ice Sheet (GrIS) is a reservoir of water highly sensitive to changes in climate (e.g. Box *et al.*, 2006; Fettweis, 2007; Hanna *et al.*, 2007, 2008, 2009). Arctic climate has warmed substantially since the end of the Little Ice Age to present (Serreze *et al.*, 2000). According to Chylek *et al.* (2006), Greenland temperatures increased during two periods with the rate of warming in 1920–1930 being about 50% higher than that in 1995–2005. Since 1957, the mean annual air temperature (MAAT) has increased more than  $2^\circ\text{C}$  for the Arctic (<http://giss.nasa.gov/>). The recent (since early 1990s) Greenland warming is strongly correlated with global warming (Hanna *et al.*, 2008). Warming has been accompanied by an increase in precipitation of approximately

1% per decade (ACIA, 2005). Assuming future greenhouse gas emissions following the A2 scenario (Nakicenovic *et al.*, 2000), climate models project increased mean annual surface air temperature by  $2.5^\circ\text{C}$  in the mid-twenty-first century and  $4.5$  to  $5.0^\circ\text{C}$  by the end of the century for areas north of  $60^\circ\text{N}$  (ACIA, 2005; IPCC, 2007).

Arctic cryospheric and hydrological responses to the altered climatic state have been reported by Abdalati and Steffen (1997); Serreze *et al.* (2000); Vorosmarty *et al.* (2001); Moritz *et al.* (2002); Hinzman *et al.* (2005); Mernild *et al.* (2008c,e), and Hanna *et al.* (2007, 2008). In Greenland, temperature changes result in a retreating ice sheet, increasing ice sheet melt extent, melting glaciers, decreasing snow cover, and increasing freshwater flux to the ocean. Melt-threshold conditions are especially sensitive. Owing to the gentle slope of the GrIS, small changes in air temperature produce large areal changes in dry and wet snow facies. Assuming an adiabatic lapse rate, a slope above the equilibrium line altitude (ELA; defined as the elevation where surface

\* Correspondence to: Sebastian H. Mernild, International Arctic Research Center and Water & Environmental Research Center, University of Alaska Fairbanks, P.O. Box 99775-0292, Fairbanks, Alaska 99775, USA.  
E-mail: fxsm@uaf.edu

mass balance, SMB, equals zero) of  $0.4^\circ$ , and a melt area perimeter of 3300 km, a  $1^\circ\text{C}$  temperature rise increases the melt area by 79 000  $\text{km}^2$  (Abdalati and Steffen, 1997).

Observations indicate that GrIS runoff has increased. Previous GrIS modelling efforts identified substantial mass losses via runoff with estimates of  $281 \text{ km}^3 \text{ y}^{-1}$  (1953–2003; Janssens and Huybrechts, 2000);  $278 \text{ km}^3 \text{ y}^{-1}$  (1988–1999; Mote, 2003);  $396 \text{ km}^3 \text{ y}^{-1}$  (1995–2004; Box *et al.*, 2006);  $304 \text{ km}^3 \text{ y}^{-1}$  (1979–2006; Fettweis, 2007); and  $351 \text{ km}^3 \text{ y}^{-1}$  (1995–2007; Hanna *et al.*, 2008). A GrIS satellite study by Tedesco (2007) indicates that the 2007 melt-index, defined as the melting area  $>2000$  m elevation multiplied by the number of melting days, set a record for snowmelt. Mote (2007) observed a large GrIS melt increase during summer 2007 that was 60% greater than the previous observed (1998) maximum. Altered runoff affects the freshwater flux to the West (Baffin Bay, Davis Strait, and Labrador Sea) and to the East (Greenland–Iceland–Norwegian Seas). Changes in freshwater flux to the ocean play an important role in determining global ocean thermohaline circulation, salinity, ice sea dynamics (e.g. Broecker *et al.*, 1985; Broecker and Denton, 1990; Su *et al.*, 2006), global eustatic sea level rise (e.g. Dowdeswell *et al.*, 1997; ACIA, 2005; Box *et al.*, 2006; IPCC, 2007), plans for hydroelectric power in Greenland (Mernild and Hasholt, 2006; Hasholt and Mernild, 2008), and the transport of sediment and nutrients from land to the ocean (e.g. Rysgaard *et al.*, 2003; Hasholt *et al.*, 2006; Hasholt and Mernild, 2006, 2008).

This study attempts to improve our quantitative understanding of the 2007 GrIS surface melt extent, a year with record GrIS surface melt extent, and contextualize it within a 1995–2007 perspective. The aim of this study is to apply a state-of-the-art modelling system, SnowModel (Liston and Elder, 2006a; Mernild *et al.*, 2006b; Liston *et al.*, 2007), to the GrIS to calculate surface hydrological processes (accumulation and ablation) and improve our quantitative understanding of the GrIS SMB and consequent freshwater flux to the ocean. GrIS model simulations were performed for 1995–2007 with the objectives of: (1) simulating inter-annual variability in surface melt extent; (2) comparing the 2007 record extent with 1995–2006 average values; (3) estimating interannual variability in the SMB components; (4) comparing 2007 SMB with 1995–2006 average SMB values; (5) contrasting SnowModel simulations with previous studies; and (6) assessing the GrIS freshwater contribution to global eustatic sea level rise.

## STUDY AREA

Greenland is 2600 km long from the northernmost point at Cape Morris Jesup ( $83^\circ\text{N}$ ) to the southern tip at Cape Farwell ( $60^\circ\text{N}$ ) (Figure 1). Greenland is dominated by the largest ice sheet in the Northern Hemisphere, the GrIS ( $1.834 \times 10^6 \text{ km}^2$ ), which covers approximately 85% of

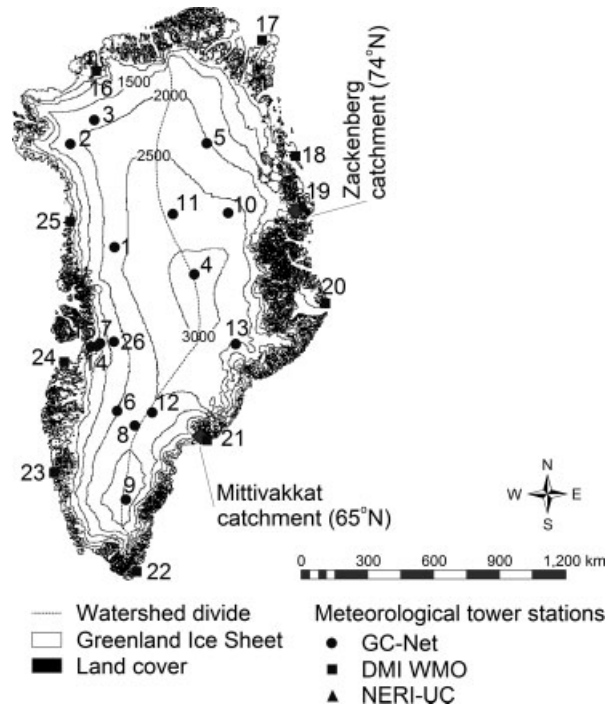


Figure 1. Greenland simulation domain with topography (500-m contour interval) including the GrIS. The location of the Mittivakkat catchment and the Zackenberg catchment, and the location of the GrIS Climate Network (GC-Net) meteorological tower stations, the coastal Danish Meteorological Institute WMO (DMI WMO) tower stations, and the meteorological tower station from Danish National Environmental Institute (NERI) and University of Copenhagen (UC) are illustrated (the numbers refer to station information in Table I)

the island. The ice sheet's maximum altitude is more than 3200 m above sea level (a.s.l.) (Figure 1). Around the margin of the GrIS is a land strip which is up to 200 km wide, is mountainous, includes numerous glaciers and ice caps, and has a number of fjords reaching the interior.

The climate in Greenland is Arctic (Born and Böcher, 2001; Mernild *et al.*, 2008d). Greenland's mean annual air temperature (MAAT) is  $-13.3^\circ\text{C}$  for the simulation period (1995–2007) (Figure 2). The MAAT increased  $\sim 1.7^\circ\text{C}$  from 1995 through 2007, with a pronounced rise of  $3.0^\circ\text{C}$  in the interior. In south and southeast Greenland, the annual precipitation is up to 2,400 mm w.eq.  $\text{y}^{-1}$ , while the northernmost areas receive less than 200 mm w.eq.  $\text{y}^{-1}$  (Figure 2). The average simulated precipitation for 1995–2007 is  $344 (\pm 18) \text{ mm w.eq. y}^{-1}$ , or  $631 (\pm 32) \text{ km}^3 \text{ y}^{-1}$ , which agrees with estimates from ice-core data (e.g. McConnell *et al.*, 2001; Bales *et al.*, 2001a,b, 2009). Annual precipitation decreased 10 mm w.eq., or  $17 \text{ km}^3$ , mostly in south-eastern Greenland (Figure 2). Greenland's characteristics cause considerable contrast in its weather conditions; complex coastal topography, elevation, distance from the coast, marginal glaciers and ice caps, and the GrIS make the climate variable over short distances.

## WATER BALANCE EQUATION

Throughout the year, different surface processes (snow accumulation, snow redistribution, sublimation, surface

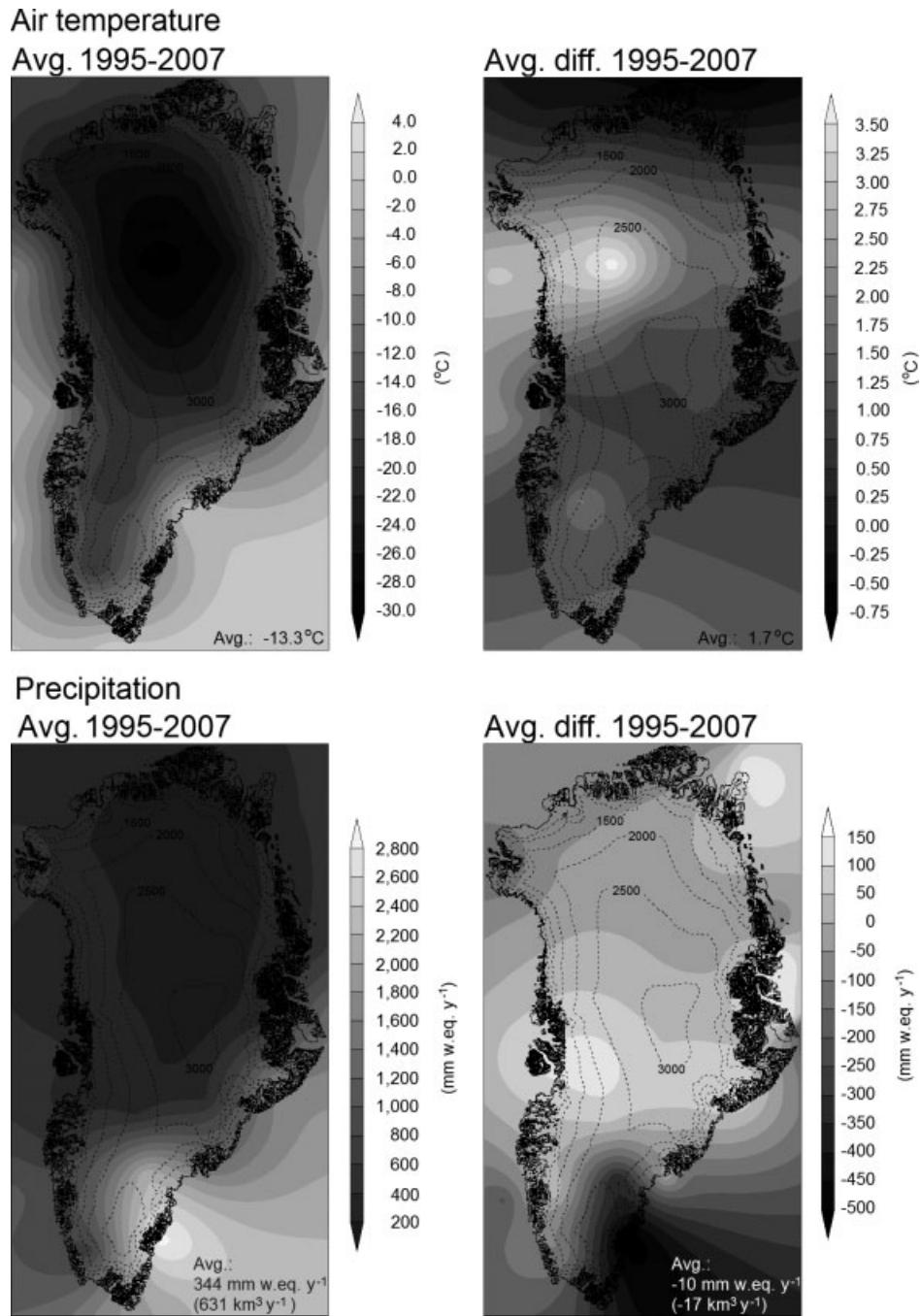


Figure 2. SnowModel simulated annual Greenland air temperature (°C) (upper row from left to right): average air temperature (1995–2007) and average annual trend difference in air temperature between 1995 and 2007; and simulated annual Greenland precipitation (mm w.eq. y<sup>-1</sup>) (lower row from left to right): average annual precipitation (1995–2007) and average annual trend difference in precipitation between 1995 and 2007

evaporation, and melting) on snow and glaciers affect glacier mass balance and high-latitude water balance (Equation (1)). The yearly water balance equation for a certain area (catchment or glacier) can be described by

$$P - (ET + SU) - R \pm \Delta S = 0 \pm \eta \quad (1)$$

where  $P$  is precipitation input from snow and rain (and possible condensation),  $ET$  is evapotranspiration (on glaciers, only evaporation occurs),  $SU$  is sublimation (including blowing-snow sublimation),  $R$  is runoff, and  $\Delta S$  is storage change (due to changes in glacier mass-balance, snow, and snow transport). The  $\Delta S$  is also

referred as surface mass-balance, SMB. Glacier storage also includes changes in supraglacial storage (lakes, pond, channels, etc.), englacier storage (ponds and the water table), and subglacier storage (cavities and lakes); glacier storage components have not been accounted for in this study. Here,  $\eta$  is the water balance discrepancy (error).

## MODELS AND METHODS

Scattered Arctic meteorological stations and limited (winter and summer) GrIS mass-balance and runoff observations have generated sparse datasets related to the spatial

and temporal distribution of snow precipitation, sublimation, GrIS surface snow and ice melt, and runoff to the ocean. Such key components are essential to hydrological research efforts, and there is a clear need to explore issues associated with data sparseness and modelling capabilities.

#### *SnowModel description*

SnowModel (Liston and Elder, 2006a) is a spatially distributed snowpack evolution modelling system specifically designed to be applicable over the wide range of snow landscapes, climates, and conditions found around the world. It is made up of four submodels: MicroMet defines the meteorological forcing conditions (Liston and Elder, 2006b); EnBal calculates the surface energy exchanges, including melt (Liston, 1995; Liston *et al.*, 1999); SnowPack simulates snow depth, water-equivalent, and snow density evolution (Liston and Hall, 1995); and SnowTran-3D is a blowing-snow model that accounts for snow redistribution by wind (Liston and Sturm, 1998, 2002; Liston *et al.*, 2007). SnowModel simulates snow-related physical processes at spatial scales ranging from 5 m to global, and temporal scales ranging from 10 min to a whole season. Simulated processes include the following: (1) accumulation and loss from snow precipitation, and blowing-snow redistribution; (2) loading, unloading, and blowing-snow sublimation; (3) snow-density, and mass transfer evolution; and (4) snowpack ripening: water equivalent, density, heat, and melt water flow and refreezing. SnowModel was originally developed for glacier-free landscapes. For glacier SMB studies on Eastern Greenland, SnowModel was modified to simulate glacier-ice melt after winter snow accumulation had ablated (Mernild *et al.*, 2006b, 2007).

At each point in the landscape, the snow evolution can be described by a snow/water mass-balance. Given the energies associated with melt and sublimation processes, mass-balance is intimately coupled to the energy balance. Changes in mass and energy balances govern the snow-cover distribution and evolution at each point in space and time, and include precipitation (solid and liquid), snowmelt, snow metamorphism (affecting factors such as density, thermal conductivity, permeability, and albedo), redistribution by wind, static-surface sublimation, blowing-snow sublimation, snowpack ripening, and snowpack meltwater runoff/retention. These processes, and their attendant impacts on snow-cover distribution and evolution, are described mathematically and combined to form a snow-evolution modelling system (Liston and Elder, 2006a,b).

*MicroMet.* MicroMet is a quasi-physically-based meteorological distribution model (Liston and Elder, 2006b) designed specifically to produce the high-resolution meteorological forcing distributions (air temperature, relative humidity, wind speed, wind direction, precipitation, solar and long-wave radiation, and surface pressure)

required to run spatially distributed terrestrial models over a wide range of landscapes in a physically realistic manner. MicroMet uses elevation-related interpolations to modify air temperature, humidity, and precipitation following Kunkel (1989); Walcek (1994); Dodson and Marks (1997), and Liston *et al.* (1999). Temperature and humidity distributions are defined to be compatible with observed lapse rates. Wind flow in complex topography is simulated following Ryan (1977) and Liston and Sturm (1998). Solar radiation variations are calculated using elevation, slope, and aspect relationships (Pielke, 2002). Incoming long-wave radiation is calculated while taking into account cloud cover and elevation-related variations following Iziomon *et al.* (2003). Precipitation is distributed following Thornton *et al.* (1997). In addition, any data from more than one location, at any given time, are spatially interpolated over the domain using a Gaussian distance-dependent weighting function and interpolated to the model grid using the Barnes objective analysis scheme (Barnes, 1964, 1973; Koch *et al.*, 1983). Liston and Elder (2006b) and Liston *et al.* (2007) performed a rigorous validation of MicroMet using various observational datasets and geographic domains. Further, MicroMet has been used to distribute observed and modelled meteorological variables over a wide variety of landscapes in the United States; Colorado (Greene *et al.*, 1999), Wyoming (Hiemstra *et al.*, 2002; 2006), Idaho (Prasad *et al.*, 2001), and Arctic Alaska (Liston *et al.*, 2002, 2007, Liston and Sturm, 1998, 2002), Norway; Svalbard and central Norway (Bruland *et al.*, 2004); East Greenland and GrIS (Mernild *et al.*, 2006a,b, 2007, 2008a,b,d,e); and near-coastal Antarctica (Liston *et al.*, 1999; Liston and Winther, 2005).

*EnBal.* EnBal performs standard surface energy balance calculations (Liston, 1995; Liston *et al.*, 1999). This component simulates surface (skin) temperatures, and energy and moisture fluxes in response to observed and/or modelled near-surface atmospheric conditions provided by MicroMet. Surface latent and sensible heat flux and snowmelt calculations are made using a surface energy balance model of the form:

$$(1 - \alpha) Q_{si} + Q_{li} + Q_{le} + Q_h + Q_e + Q_c = Q_m \quad (2)$$

where  $Q_{si}$  is the solar radiation reaching earth's surface,  $Q_{li}$  is the incoming long-wave radiation,  $Q_{le}$  is the emitted long-wave radiation,  $Q_h$  is the turbulent exchange of sensible heat,  $Q_e$  is the turbulent exchange of latent heat,  $Q_c$  is the conductive energy transport,  $Q_m$  is the energy flux available for melt, and  $\alpha$  is the surface albedo. Details of each term in Equation (2), and the model solution, are available in Liston (1995) and Liston *et al.* (1999). In the presence of snow or glacier ice, surface temperatures greater than 0 °C indicate that energy is available for melting. This energy is computed by fixing the surface temperature at 0 °C and solving Equation (2) for  $Q_m$ . Energy transports toward the surface are defined to be positive.

*SnowPack.* SnowPack is a single-layer, snowpack-evolution and runoff/retention model that describes snowpack changes in response to precipitation and melt fluxes defined by MicroMet and EnBal (Liston and Hall, 1995; Liston and Elder, 2006a). Its formulation closely follows Anderson (1976). In SnowPack, the density changes with time in response to snow temperature and weight of overlying snow (Liston and Elder, 2006a). A second density-modifying process results from snow melting. The melted snow reduces the snow depth and percolates through the snowpack. If snow temperature is below freezing, any percolating/liquid water refreezes and is stored in the snow (in the 'pores') as internal refreezing. When saturated snow density, assumed to be  $550 \text{ kg m}^{-3}$  (Liston and Hall, 1995), is reached, actual runoff occurs. This provides a method to account for heat and mass transfer processes, such as snowpack ripening, during spring melt. The density of new snow from additional accumulation is defined following Anderson (1976) and Liston and Hall (1995). Static-surface (nonblowing snow) sublimation calculated in EnBal is used to adjust the snowpack depth; blowing-snow sublimation is calculated in SnowTran-3D (Liston and Elder, 2006a).

*SnowTran-3D.* SnowTran-3D (Liston and Sturm, 1998; Liston *et al.*, 2007) is a three-dimensional submodel that simulates snow depth evolution (deposition and erosion) resulting from windblown snow based on a mass-balance equation that describes the temporal variation of snow depth at each grid cell within the simulation domain. SnowTran-3D's primary components are a wind-flow forcing field, a wind-shear stress on the surface, snow transport by saltation, snow transport by turbulent suspension, sublimation of saltating and suspended snow, and accumulation and erosion at the snow's surface (Liston and Sturm, 2002). Simulated transport and blowing-snow sublimation processes are influenced by the interactions among available snow, topography, and atmospheric conditions (Liston and Sturm, 1998). SnowTran-3D simulates snow depth evolution, and then uses the snow density simulated by SnowPack to convert to the more hydrologically significant snow-water equivalent (SWE) depth. Deposition and erosion, which lead to changes in snow depth (Equation (3)), are the result of changes in horizontal mass-transport rates of saltation,  $Q_{salt}$  ( $\text{kg m}^{-1} \text{ s}^{-1}$ ), changes in horizontal mass-transport rates of turbulent suspended snow,  $Q_{turb}$  ( $\text{kg m}^{-1} \text{ s}^{-1}$ ), sublimation of transported snow particles,  $Q_v$  ( $\text{kg m}^{-2} \text{ s}^{-1}$ ), and the water-equivalent precipitation rate,  $P$  ( $\text{m s}^{-1}$ ). Combined, the time rate of change in snow depth,  $\zeta$  (m), is

$$\frac{d(\rho_s \zeta)}{dt} = \rho_w P - \left( \frac{dQ_{salt}}{dx} + \frac{dQ_{turb}}{dx} + \frac{dQ_{salt}}{dy} + \frac{dQ_{turb}}{dy} \right) + Q_v \quad (3)$$

where  $t$  (s) is time;  $x$  (m) and  $y$  (m) are the horizontal coordinates in the west–east and south–north directions, respectively; and  $\rho_s$  and  $\rho_w$  ( $\text{kg m}^{-3}$ ) are snow and water

density respectively. At each time step, Equation (3) is solved for each individual grid cell within the domain, and is coupled to the neighboring cells through the spatial derivatives ( $d/dx$ ,  $d/dy$ ). SnowTran-3D simulations have previously been compared against observations in glacier and glacier-free alpine, Arctic, and Antarctic landscapes (Greene *et al.*, 1999; Liston *et al.*, 2000, 2007; Prasad *et al.*, 2001; Hiemstra *et al.*, 2002, 2006; Liston and Sturm, 2002; Bruland *et al.*, 2004; Mernild *et al.*, 2006a,b, 2007, 2008a,b,d,e).

#### *SnowModel input*

To solve this system of equations, SnowModel requires spatially distributed fields of topography and land cover, and temporally distributed point meteorological data (air temperature, relative humidity, wind speed, wind direction, and precipitation) obtained from meteorological stations located within the simulation domain. For this study, data were obtained from 26 meteorological stations: 16 stations from the Greenland Climate Network (GC-Net), 9 WMO stations operated by the Danish Meteorological Institute (DMI), and 1 by the Danish National Environmental Research Institute and University of Copenhagen (Figure 1 and Table I).

Snow precipitation measurements include uncertainties, especially under windy and cold conditions (e.g. Yang *et al.*, 1999; Liston and Sturm, 2002, 2004; Serreze and Barry, 2005). Solid and liquid precipitation measurements at the DMI meteorological stations (Figure 1 and Table I; stations 16–18 and 20–25) were calculated from Helman–Nipher shield observations corrected according to Allerup *et al.* (1998, 2000). Solid (snow) precipitation was calculated from snow-depth sounder observations at the other stations (Figure 1 and Table I) after the sounder data noise was removed; these data are assumed to be accurate within  $\pm 10$ – $15\%$  (Mernild *et al.*, 2007). Snow depth sounder observations were partitioned into liquid (rain) precipitation and solid (snow) precipitation at different air temperatures based on methods employed at Svalbard (Førland and Hanssen-Bauer, 2003). For air temperatures below  $-1.5^\circ\text{C}$ , sounder data were considered to represent solid precipitation, and for temperatures above  $3.5^\circ\text{C}$  precipitation is considered liquid; linear interpolation calculated snow and rain fractions at temperatures between these limits. Snow-depth increases at relative humidity  $< 80\%$  and at wind speed  $> 10 \text{ m s}^{-1}$  were removed to better distinguish between the proportions of real snow accumulation based on precipitation events and blowing snow redistribution (Mernild *et al.*, 2007). Remaining snow-depth increases were adjusted using a temperature-dependent snow density (Brown *et al.*, 2003) and hourly snowpack settling.

Simulations were performed on a daily time step. However, blowing snow and snow- and ice-melt are threshold processes that may not be accurately represented at this time step. Therefore, daily simulated melt and blowing-snow processes were compared against hourly simulated values from a smaller test area, the Mittivakkat Glacier

Table I. Meteorological input data for the Greenland SnowModel simulations

Meteorological station number	Meteorological station name	Location: (degrees and minutes)	Data time period (year, month, and day)	Altitude (m a.s.l.)
1	NASA-U	73°50'31"N; 49°29'54"W	1998-1-1 to 2006-4-26	2369
2	GITS	77°08'16"N; 61°02'24"W	1999-5-7 to 2007-5-3	1869
3	Humboldt	78°31'36"N; 56°49'50"W	1998-1-2 to 2007-5-3	1995
4	Summit	72°34'47"N; 38°30'18"W	1999-9-1 to 2007-5-2	3208
5	Tunu-N	78°00'59"N; 33°59'00"W	1996-5-17 to 2007-31-12	2052
6	DYE-2	66°28'48"N; 46°16'44"W	1996-5-25 to 2007-4-25	2165
7	JAR1	69°29'51"N; 49°41'16"W	1996-6-20 to 2007-5-10	962
8	Saddle	65°59'58"N; 44°30'03"W	1997-4-20 to 2007-4-24	2456
9	South Dome	63°08'56"N; 44°49'02"W	1996-4-23 to 2004-10-12	2901
10	NASA-E	75°00'02"N; 29°59'50"W	1997-5-3 to 2006-5-3	2614
11	NGRIP	75°05'59"N; 42°19'57"W	1997-7-9 to 2005-12-31	2950
12	NASA-SE	66°28'45"N; 42°29'56"W	1998-4-24 to 2007-2-17	2393
13	KAR	69°41'58"N; 33°00'21"W	1998-5-18 to 2005-6-7	2579
14	JAR2	69°25'09"N; 50°03'55"W	1999-6-2 to 2006-5-7	542
15	JAR3	69°23'40"N; 50°18'36"W	2001-1-1 to 2004-5-24	283
16	Hall Land	81°41'00"N; 59°57'00"W	1995-1-1 to 1996-8-31	105
17	Station Nord	81°36'00"N; 16°39'00"W	1995-1-1 to 2007-12-31	36
18	Danmarkshavn	76°46'00"N; 18°40'00"W	1995-1-1 to 2007-12-31	11
19	Zackenbergl	74°28'10"N; 20°34'20"W	1997-9-1 to 2007-12-31	43
20	Ittoqqortoormiit	70°29'00"N; 21°57'00"W	1995-1-1 to 2007-12-31	66
21	Tasiilaq	65°36'00"N; 37°38'00"W	1995-1-1 to 2007-12-31	44
22	Ikerassuaq	60°03'00"N; 43°10'00"W	1995-1-1 to 2007-12-31	88
23	Nuuk	64°10'00"N; 51°45'00"W	1995-1-1 to 2007-12-31	80
24	Aasiaat	68°42'00"N; 52°45'00"W	1995-1-1 to 2007-12-31	88
25	Kitsissorsuit	74°02'00"N; 57°49'00"W	1995-1-1 to 2007-12-31	40
26	Swiss Camp	69°34'03"N; 49°19'17"W	1995-1-1 to 2006-16-8	1140

Meteorological station data on the GrIS (Station numbers 1–15, and 26) were provided by the Cooperative Institute for Research in Environmental Science (CIRES), University of Colorado at Boulder, coastal meteorological station data (Station numbers 16–18, and 20–25) by the Danish Meteorological Institute (DMI), and the Zackenberg meteorological station (Station number 19) by the Danish Polar Center (DPC), the Greenland Survey (ASIAQ), and the GeoBasis [Danish National Environmental Research Center (NERI) and the Department of Geography and Geology, University of Copenhagen (IGUC)].

(31 km<sup>2</sup>), SE Greenland (Mernild and Liston, 2009). Glacier winter, summer, and net mass-balances significantly ( $p < 0.01$ ) differed 2%, 3%, and 8%, respectively. We also recognize that daily-averaged atmospheric forcing variables, in contrast to hourly data, smoothed the meteorological driving data. Further examination of these climate-cryospheric scaling issues will be studied at the GrIS Kangerluassuaq drainage area, West Greenland, in order to better estimate freshwater influx to the ocean.

Greenland topographic data for the model simulations were provided by Bamber *et al.* (2001) who applied “correction” elevations derived by satellite imagery to an existing radar-altimetry digital elevation model (DEM). The image-derived correction was determined from a high-resolution (625 m) grid of slopes inferred from the regional slope-to-brightness relationship of 44 AVHRR images covering all of Greenland (Scambos and Haran, 2002). For the model simulations, this DEM was aggregated to a 5-km grid-cell increment and clipped to yield a 2830 by 1740 km simulation domain that encompassed all of Greenland. The GrIS terminus was confirmed or estimated by using aerial photos and maps (1:250,000 Geodetic Institute, Denmark).

Each grid cell within the domains was assigned a USGS Land Use/Land Cover System class according to the North American Land Cover Characteristics Database, Version 2.0 (available on-line at [http://

edcdaac.usgs.gov/glcc/na\_int.html] from the USGS EROS Data Center’s Distributed Active Archive Center, Sioux Falls, South Dakota, USA). The snow-holding depth (the snow depth that must be exceeded before snow can be transported by wind) was assumed to be constant. Albedo was assumed to be 0.8 for snow (Table II). Realistically, snow albedo changes with time and surface characteristics (Pomeroy and Brun, 2001); thus, the model likely underestimates the energy available for surface melting. When the snow is ablated, the GrIS surface ice conditions are used. Albedo was assumed to be 0.4 for ice; however, the GrIS ablation zone is characterized by lower albedo on the margin and an increase in albedo toward the ELA, where a veneer of ice and snow dominate the surface (Boggild *et al.*, 2006). The emergence and melting of old ice in the ablation zone creates surface layers of dust (black carbon particles) that were originally deposited with snowfall higher on the ice sheet. This debris cover is often augmented by locally derived windblown sediment. Particles on or melting into the ice change the area-average albedo, increasing melt. User-defined constants for SnowModel are shown in Table II (for parameter definitions see Liston and Sturm, 1998, 2002).

Various Greenland cryospheric processes were not represented in the model. All fjord and ocean areas within the domain were excluded from model simulations. Also,

Table II. User-defined constants used in the SnowModel simulations (see Liston and Sturm (1998) for parameter definitions)

Symbol	Value	Parameter
$C_v$		Vegetation snow-holding depth (equal surface roughness length) (m)
	0.50	Barren
	0.15	Grassland
	1.00	Mixed forest
	0.50	Mixed tundra
	0.30	Shrubland
	0.01	Snow
	0.01	Ice
	0.50	Wooded tundra
	0.50	Wooded wetland
	0.01	Water (ocean and lake)
	$f$	500.0
$U_{*t}$	0.25	Threshold wind-shear velocity ( $\text{m s}^{-1}$ )
$dt$	1	Time step (day)
$Dx = dy$	5.0	Grid cell increment (km) Greenland simulation area
$\alpha$		Surface albedo
	0.8	Snow
	0.4	Ice
$\rho$		Surface density ( $\text{kg m}^{-3}$ )
	280	Snow
	910	Ice
$\rho_s$	550	Saturated snow density ( $\text{kg m}^{-3}$ )

changes in glacier storage based on supraglacial storage (lakes, pond, channels, etc.), englacial storage (ponds and the water table), subglacial storage (cavities and lakes), melt water routing, and changes based on iceberg calving are not calculated in SnowModel, even though they might influence runoff.

#### SnowModel validation and uncertainty

Few validation observations for *in situ* snow-evolution, snow and ice surface melt, and glacier net mass-balance are available in Greenland. Therefore, SnowModel accumulation and ablation routines were tested qualitatively (by visual inspection) and quantitatively (cumulative values and linear regression) using independent *in situ* observations on snow pit depths; glacier winter, summer, and net mass-balances; depletion curves; photographic time lapses; and satellite images from the Mittivakkat ( $65^\circ\text{N}$ ) and Zackenberg ( $74^\circ\text{N}$ ) glacier catchments, East Greenland (Figure 1). A comparison between simulated and observed values from the two glacier catchments indicates a 7% maximum difference between modelled and observed snow depths, glacier mass-balance, and snow cover extent (Table III) (for further details see Mernild *et al.*, 2006a,b, 2007). On the basis of this adequate performance, SnowModel routines were adjusted to run over the entire GrIS to simulate water balance components (Equation (1)), including runoff to the ocean.

To assess the model performance for the GrIS, SnowModel/MicroMet was validated with independent station data (1995 through 2005), satellite observations, and comparisons with other studies (e.g. Mernild *et al.*,

2008a,b). First, SnowModel/MicroMet distributed meteorological data were compared against independent meteorological station data. The Swiss Camp Station (Figure 1 and Table I; Station #26), located on the GrIS and 40 km from the nearest simulation station (JAR1; Station #7), was used for assessment. MicroMet-simulated meteorological data were correlated with observed data. Simulated air temperature, relative humidity, and precipitation values account for 84%, 63%, and 69% of the variance in the observed daily-averaged dataset. Wind speed had less strong correlations (50%), but remained respectable (Mernild *et al.*, 2008a). This comparison is limited because it employs only one independent station (meteorological stations are a rare commodity in this area and throughout the Arctic); however, we assume that MicroMet satisfactorily represents GrIS meteorological conditions. Second, SnowModel simulated melt extents were compared against concurrent passive microwave satellite-derived melt extent, indicating a 1995–2005 average difference of 4% (Table III) (Mernild *et al.*, 2008a,b). The satellite-derived melt extent (melting ice and wet snow areas) was integrated over an entire melt season based on a 25-km grid-cell increment (Abdalati and Steffen, 1997). The criterion for satellite-derived melt was 1% mean liquid water content by volume in the top meter of snow. The melting threshold of the XGPR microwave algorithm did not show any melt in the centre part of the GrIS, and this roughly corresponded with SnowModel simulations of snowmelt. Third, SnowModel simulated melt-index (above the 2000-m GrIS contour line) was consistent with observations by Tedesco (2007); Mernild *et al.* (2008a). In addition, SnowModel-simulated ELA was validated against an ELA-parameterization by Zwally and Giovinetto (2001) for the East and West GrIS; the average and maximum difference was 35 m a.s.l. and 425 m a.s.l. respectively (Table III). The maximum difference may be due to the great distance between East Greenland meteorological stations.

SnowModel/MicroMet adequately simulated the spatial distribution of meteorological parameters (wind speed, air temperature, relative humidity, and precipitation) and snow accumulation and ablation processes with respect to existing observations and studies (Table III). Model uncertainties are largely determined by processes not yet represented by standard routines in the modelling system: e.g. routines for simulating the temperature inversion layer and variable albedo, and changes in glacier area, size, and height according to glacier dynamic processes.

## RESULTS AND DISCUSSION

Satellite observed and SnowModel end-of-summer melt extent was lowest (29%;  $0.529 \times 10^6 \text{ km}^2$ ) in 1996 and highest (51%;  $0.915 \times 10^6 \text{ km}^2$ ) in 2007 (Figure 3). In 1996 and 2007, surface melt occurred at elevations as high as 2550 and 2980 m a.s.l. respectively (Figure 3),

Table III. Different SnowModel validation studies from East Greenland: the Mittivakkat Glacier catchment (65°N), the Zackenberg Glacier catchment (74°N), and from the GrIS

Validation of SnowModel routines against observations and other studies on Greenland				
	Parameter	Discrepancy between modelled and observed	Time period	Reference for model study
Mittivakkat Glacier catchment, East Greenland, (65°N)	SWE depth:- average	Maximum 1%	May 1997/98	Hasholt <i>et al.</i> , 2003
	Snow depth:- point	Maximum 7%	Aug 2004 and May/June 2005	Mernild <i>et al.</i> , 2006b
	The Mittivakkat Glacier:		1999/2000 to 2003/04	Mernild <i>et al.</i> , 2006b
	- Winter mass-balance	Maximum 4%		
	- Summer mass-balance	Maximum 7%		
	- Glacier net mass-balance	Maximum 3%		
	Location of ELA	Maximum 100 m a.s.l.	1998/99 to 2005/06	Mernild <i>et al.</i> , 2006b, 2008e
Zackenberg Glacier catchment, East Greenland, (74°N)	Average end-of-winter SWE depth	Maximum 6%	2004 and 2005	Mernild <i>et al.</i> , 2007, 2008d
	Snow extent base on depletion curves	Maximum 5%	2000 to 2002	Mernild <i>et al.</i> , 2007, 2008d
	Snow extent based on satellite image	7%	June 2002	Mernild <i>et al.</i> , 2007
Greenland Ice Sheet (GrIS)	Average meteorological data:	1995 to 2005	Mernild <i>et al.</i> , 2008a	
	- Air temperature	0.2 °C		
	- Wind Speed	0.2 m s <sup>-1</sup>		
	- Relative humidity	0.1%		
	- Precipitation	1.0 mm w.eq		
	End-of-season satellite-derived surface melt extent	Average 4% and maximum distance of 160 km between modeled and satellite-observed melt and nonmelt boundaries	1995 to 2005	Mernild <i>et al.</i> , 2008a,b
Melt-Index	Modeled results are consistent with observations	1995 to 2005	Mernild <i>et al.</i> , 2008a	
	Location of ELA	Average 35 m a.s.l. and maximum 425 m a.s.l.	1995 to 2005	Mernild <i>et al.</i> , 2008a

The location of the Mittivakkat and the Zackenberg Glacier catchments are illustrated on Figure 1

and the modelled 2007 melt extent was 80% greater than the modelled 1996 extent. The year 1996 featured an average temperature anomaly of  $-0.40$ , while that of 2007 was  $0.38$  (Table III). For 1995–2007, simulated changes in the GrIS end-of-summer surface snow and ice melt extent showed the greatest melt extent increase in the southern part of the GrIS. This was probably due to a combination of relatively lower latitude, altitude, and surface slope. In 2007, the melt extent entirely dominated the southern part of the GrIS (below 66°N) (Figure 3). To the north, interannual melt changes are less pronounced. On average, the simulated melt area increased  $\sim 8\%$  ( $\sim 127\,000$  km<sup>2</sup>; linear regression) in size from 1995 through 2007. This change correlated to the average increase ( $R^2 = 0.66$ ,  $p < 0.01$ , linear regression) in MAAT of  $\sim 1.7$  °C. In the 13-year series (1995–2007), 2007, 2005, 2002, and 1998 were the first-, second-, third-, and fourth-highest melt extent years.

For 2007—the year with the highest ablation—the surface melt extent of  $0.915 \times 10^6$  km<sup>2</sup> is around 20% greater than average of  $0.752 \times 10^6$  km<sup>2</sup> for the period 1995–2006.

Modelled and satellite-derived nonmelt distributions are similar. In some areas, the discrepancy distance can be up to 160 km, especially in the northern and northeastern part of the GrIS (Figure 3), where the distance among the meteorological stations is great (Mernild *et al.*, 2009). Modelled nonmelt areas of the GrIS are, on average, underestimated by 1% for 1996 and 4% for 2007, according to satellite-derived melt observations (Figure 3). This indicates a strong correlation between modelled and satellite-derived melt extent. This discrepancy might be partially due to issues surrounding the one-day simulation time step and scaling mismatch with the 25-km grid-cell increment of the satellite melt observations.

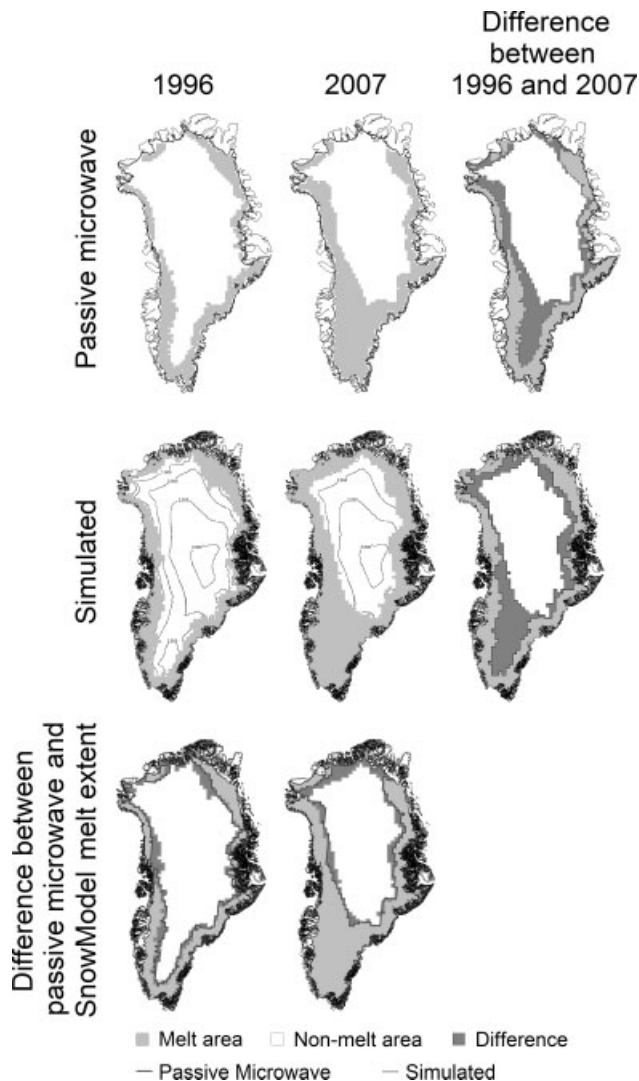


Figure 3. The GrIS melt extent based on passive microwave satellite-derived observations and SnowModel simulations for the years 1996 (the year with the lowest melt area) and 2007 (the year with the greatest melt area). Furthermore, the difference between satellite-derived and SnowModel simulations melt extent from 1996 and 2007 are illustrated. Topography (500-m contour interval) is included on the 1996 and 2007-simulated output to illustrate the height of the surface melt extent. The satellite-derived melt extent is based on data provided by the Cooperative Institute for Research in Environmental Sciences (CIRES), University of Colorado at Boulder

Modelled surface water balance components  $P$ ,  $ET$ ,  $SU$ ,  $R$ , and  $\Delta S$  (Equation (1)) are presented in Figure 4 for the GrIS from 1995 through 2007. The SMB ( $\Delta S$ ) is governed by an integrated accumulation (snow precipitation) and ablation (evaporation, sublimation, and runoff) over the GrIS. Statistically significant relationships exist between SMB and precipitation ( $R^2 = 0.41$ ,  $p < 0.01$ ) and SMB and ablation ( $R^2 = 0.86$ ,  $p < 0.01$ ), indicating that SMB fluctuations were largely tied to ablation processes. Throughout the simulation period, SMB varied from  $-3$  (2007) to  $310 \text{ km}^3 \text{ y}^{-1}$  (1996), averaging  $124 (\pm 83) \text{ km}^3 \text{ y}^{-1}$  (Table IV). For the 1995–2007 simulations, 2004, 1995, 1998, and 2005 were the first-, second-, third-, and fourth-lowest precipitation years, and 2007, 1998, 2003, and 2002 were the first-, second-,

third-, and fourth-highest runoff years. The years 2007, 1998, 2003, and 1995 were first-, second-, third-, and fourth-lowest SMB. During the simulation period, SMB values near, or below, zero occur for 1998 ( $2 \text{ km}^3 \text{ y}^{-1}$ ) and 2007 ( $-3 \text{ km}^3 \text{ y}^{-1}$ ) (Table IV). Relatively high ablation values occurred in 1998 ( $597 \text{ km}^3 \text{ y}^{-1}$ ; 81% was runoff) and 2007 ( $627 \text{ km}^3 \text{ y}^{-1}$ ; 83% was runoff); 1998 and 2007 also featured relatively low precipitation values of 598 and  $624 \text{ km}^3 \text{ y}^{-1}$  respectively (Figure 4). The 2007 runoff of  $523 \text{ km}^3 \text{ y}^{-1}$  was around 35% greater than the average of  $389 \text{ km}^3 \text{ y}^{-1}$  for 1995–2006. The 2007 precipitation of  $624 \text{ km}^3 \text{ y}^{-1}$  was 6% lower than average of  $664 \text{ km}^3 \text{ y}^{-1}$  for the period 1995–2006 (Table IV and Figure 4). A combination of higher runoff and lower precipitation than average created the record negative 2007 SMB value of  $-3 \text{ km}^3 \text{ y}^{-1}$  (Table IV).

Precipitation was more uniform while runoff increased (Figure 4), leading to enhanced average SMB loss of  $127 \text{ km}^3$  (linear regression  $R^2 = 0.24$ ,  $p < 0.05$ ). A regression of the 13-year precipitation amount indicated no significant trend ( $R^2 = 0.03$ ,  $p < 0.25$ , linear regression). The fraction of liquid precipitation rose  $9 \text{ km}^3 \text{ y}^{-1}$  ( $R^2 = 0.26$ ,  $p < 0.025$ ), from  $26 \text{ km}^3 \text{ y}^{-1}$  (4% of total precipitation) in 1995 to  $35 \text{ km}^3 \text{ y}^{-1}$  (6%) in 2007. Ablation rose  $110 \text{ km}^3$  ( $R^2 = 0.27$ ,  $p < 0.05$ ) and runoff increased  $104 \text{ km}^3$  ( $R^2 = 0.26$ ,  $p < 0.05$ ). Only 9% of the runoff increase occurs from the change in fraction of liquid precipitation; increased runoff is largely due to changes in ablation (increasing temperature). The mean annual runoff for the period 1995 through 2007 of  $399 (\pm 66) \text{ km}^3 \text{ y}^{-1}$  equals a specific runoff of  $6.9 (\pm 1.2) \text{ l s}^{-1} \text{ km}^{-2} \text{ y}^{-1}$ . Approximately 42% of the GrIS runoff drains from the East GrIS and 58% from the West GrIS.

The GrIS interior, especially in the north, had positive SMB values of  $200 \text{ mm w.eq. y}^{-1}$ , averaging  $57 (\pm 28) \text{ mm w.eq. y}^{-1}$  (Figure 5). The lowest SMB values occurred in the southwestern GrIS with up to  $-3,000 \text{ mm w.eq. y}^{-1}$ . The highest SMB values, above  $1000 \text{ mm w.eq. y}^{-1}$ , were in the southeastern GrIS. Storm tracks determine the distribution of precipitation across Greenland (e.g. Hansen *et al.*, 2008): In southeastern GrIS, precipitation increases and overwhelms ablation due to the passage of low pressure systems typically tracking southwest to northeast (Fettweis, 2007).

The ELA provides a useful metric of accumulation and ablation's net influence on the SMB. Modelled ELA changes according to topography and latitude. As latitude increases, ELA decreases in elevation. On the West GrIS, ELA varies from 900 to 1000 m a.s.l. in the north to around 1700–1800 m a.s.l. in the south. On the East GrIS, ELA is located at lower elevations from 1400–1600 m a.s.l. in the south to 600–700 m a.s.l. in the north (Figure 5). SnowModel-simulated ELA elevation for both West and East GrIS is consistent with studies by Box and Bromwich (2004) and Fettweis (2007).

SnowModel runoff routines for GrIS surface runoff take retention and internal refreezing into account when

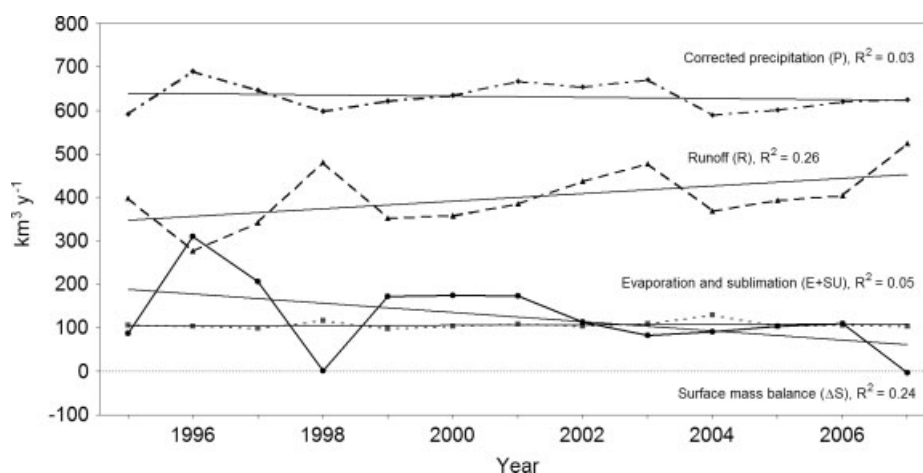


Figure 4. The 1995–2007 modelled GrIS precipitation ( $P$ ), evaporation ( $E$ ), sublimation ( $SU$ ), runoff ( $R$ ), and changes in surface mass-balance ( $\Delta S$ ), including trend lines (linear regression)

Table IV. Rank-ordered GrIS precipitation ( $P$ ), runoff ( $R$ ), surface mass-balance ( $\Delta S$ ), and air temperature anomaly for 1995 through 2007

Rank	Corrected precipitation ( $P$ ), $\text{km}^3 \text{y}^{-1}$	Runoff ( $R$ ), $\text{km}^3 \text{y}^{-1}$	Surface mass-balance ( $\Delta S$ ), $\text{km}^3 \text{y}^{-1}$	Air temperature anomaly, $^{\circ}\text{C}$
1	690 (1996)	523 (2007)	310 (1996)	1.05 (2005)
2	669 (2003)	481 (1998)	205 (1997)	0.86 (2003)
3	666 (2001)	477 (2003)	174 (2000)	0.38 (2007)
4	653 (2002)	436 (2002)	173 (2001)	0.38 (2002)
5	646 (1997)	404 (2006)	172 (1999)	0.37 (2006)
6	635 (2000)	398 (1995)	113 (2002)	0.36 (2000)
7	624 (2007)	392 (2005)	109 (2006)	0.21 (2004)
8	622 (1999)	385 (2001)	103 (2005)	-0.12 (2001)
9	619 (2006)	369 (2004)	91 (2004)	-0.25 (1998)
10	600 (2005)	358 (2000)	87 (1995)	-0.40 (1996)
11	598 (1998)	352 (1999)	83 (2003)	-0.82 (1999)
12	591 (1995)	341 (1997)	2 (1998)	-0.84 (1997)
13	589 (2004)	277 (1996)	-3 (2007)	-1.21 (1995)
Average and standard deviation	$631 \pm 32$	$397 \pm 62$	$124 \pm 83$	$0 \pm 0.68$

meltwater penetrates through the snowpack. These routines do have a significant effect on the runoff (Mernild *et al.*, 2008b). Not including retention/refreezing routines in SnowModel would lead to an overestimation of runoff to the ocean, and a consequent overestimation of the global sea level rise. If no retention/refreezing routines were included in SnowModel, 1995–2007 runoff is overestimated by 21%. An average value of 21% is in accordance with previous values of approximately 25% estimated by Janssens and Huybrechts (2000) single-layer snowpack model (used by e.g. Hanna *et al.*, 2002, 2005, 2008). The snowpack model in SnowModel is similar to the one used by Janssens and Huybrechts (2000); it does not calculate vertical temperature changes through the snowpack. For the GrIS, SnowModel retention and refreezing routines indicate that high runoff years are synchronous with low precipitation/accumulation years ( $R^2 = -0.20$ ,  $p < 0.10$ ). This trend was reported for the GrIS by Hanna *et al.* (2008), as more melt water was retained in the thicker snowpack, reducing runoff. This effect is most pronounced above the ELA where melt water does not infiltrate far into the snowpack because

of the snowpack's cold content—even during summer. Snowpack meltwater refreeze has a much smaller impact compared to coarse-scale melt in the ablation area from snow and glacier ice, and is probably within the uncertainties of the ablation region runoff model estimates.

This study's, Box *et al.*'s (2006), and Hanna *et al.*'s (2008) simulated GrIS precipitation, runoff, and surface mass-balance for the GrIS since 1995 are shown in Figure 6a–c. Similar precipitation and interannual trends were found by the three studies. SnowModel simulated precipitation was  $22 \text{ km}^3 \text{y}^{-1}$  (3%) lower than Box *et al.*'s (2006) estimate for 1995–2004 and  $14 \text{ km}^3 \text{y}^{-1}$  (2%) lower than Hanna *et al.*'s (2008) calculations 1995–2007. Snow precipitation measurements typically include uncertainties, especially under windy and cold Arctic conditions (e.g. Yang *et al.*, 1999; Liston and Sturm, 2002, 2004; Serreze and Barry, 2005). Snowfall in the Arctic is most often connected with strong winds, and typically takes the form of fine snowflakes (Sturm *et al.*, 1995). As a result, wind easily lifts and redistributes the snowflakes according to exposure and local topography, and it is sometimes difficult to distinguish between a

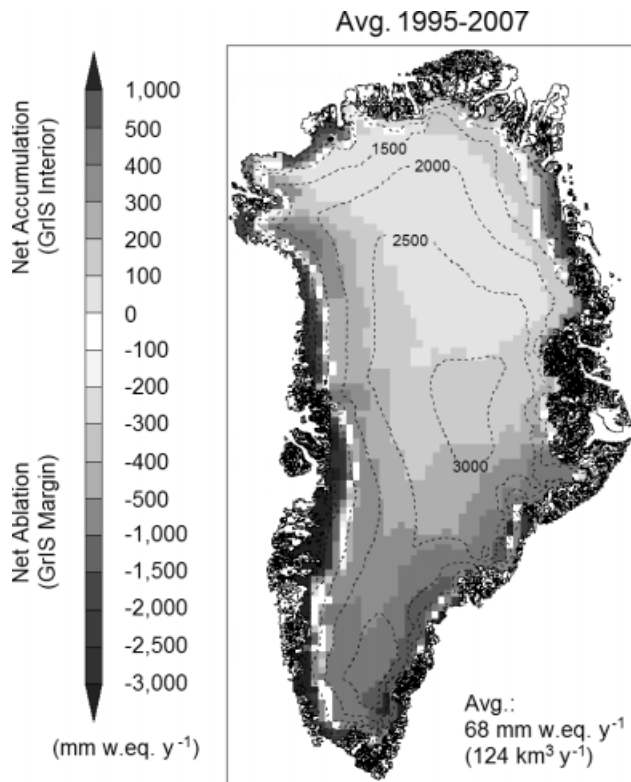


Figure 5. The 1995–2007 average modelled spatial GrIS surface mass-balance ( $\text{mm w.eq. y}^{-1}$ ), with 500-m contour interval. The 0  $\text{mm w.eq. y}^{-1}$  level is defined as the elevation where the SMB equals zero, and where the ELA occurs

period of snowfall and a period of drifting snow. Given the uncertainties in measuring snow precipitation and the limited sources of snow data, the interannual variability between SnowModel, Box *et al.* (2006) and Hanna *et al.* (2008) is expected to be similar (Figure 6a).

SnowModel GrIS runoff was  $9 \text{ km}^3 \text{ y}^{-1}$  (2%) lower than Box *et al.*'s (2006) 1995–2004 value and  $49 \text{ km}^3 \text{ y}^{-1}$  (14%) higher than Hanna *et al.*'s (2008) 1995–2007 estimate (Figure 6b). The average GrIS runoff estimated from the three approaches differ less than 15%, whether the surface melt (the potential runoff) is based on the positive degree day approach (Hanna *et al.*, 2008) or the energy balance calculations (Box *et al.*, 2006). The interannual trends are nearly identical for the three studies (Figure 6b).

SnowModel SMB from 1995 to 2004 was  $19 \text{ km}^3 \text{ y}^{-1}$  (12%) lower than that of Box *et al.* (2006). For 1995–2007, SnowModel SMB was  $171 \text{ km}^3 \text{ y}^{-1}$  (58%) lower than that of Hanna *et al.* (2008) (Figure 6c). Lower SnowModel simulated GrIS SMB values are likely due to incorporation of evaporation and sublimation values of  $107 \text{ km}^3 \text{ y}^{-1}$  in the SMB calculations (see Equation (1)). The average sublimation is  $52 \text{ km}^3 \text{ y}^{-1}$ . SnowModel simulated evaporation and sublimation accounted for 21% for the total GrIS ablation losses, and ranged from  $98 \text{ km}^3 \text{ y}^{-1}$  in 1999 to  $129 \text{ km}^3 \text{ y}^{-1}$  in 2004.

Processes not simulated in SnowModel, including subglacial geothermal bottom (basal) melting and iceberg calving, likely contributed to errors in GrIS volume mass

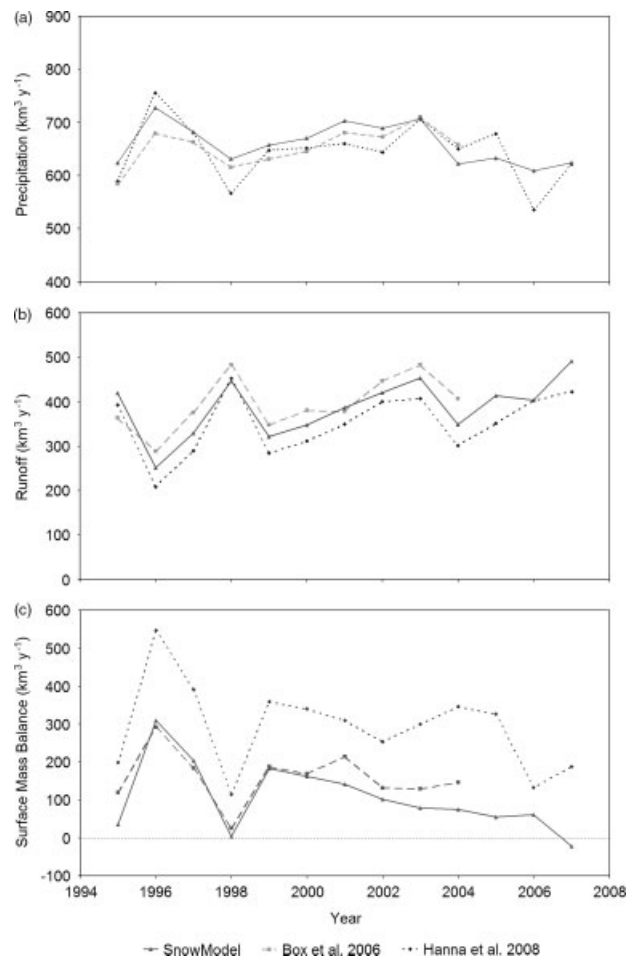


Figure 6. The 1995–2007 SnowModel, Box *et al.* (2006), and Hanna *et al.* (2008) simulated GrIS; (a) precipitation ( $P$ ); (b) runoff ( $R$ ); and (c) surface mass-balance ( $\Delta S$ )

balance estimates. As a result, this study may possess a higher uncertainty than the expected 7%. Challenges in estimating GrIS bottom melting and GrIS iceberg calving are formidable, and are derived from countless floating glacier ice tongues such as Helheim (East Greenland), Kangerdlugssuaq (East Greenland), and Jakobshavn glacier tongues (West Greenland). Reeh *et al.* (1999) and Church *et al.* (2001) estimated the bottom melting to be  $35 \text{ km}^3 \text{ y}^{-1}$  and  $32 \pm 3 \text{ km}^3 \text{ y}^{-1}$  respectively. Therefore, already published constant values for GrIS bottom melting ( $32 \pm 3 \text{ km}^3 \text{ y}^{-1}$ ; Church *et al.*, 2001) and iceberg calving ( $357 \text{ km}^3 \text{ y}^{-1}$ ; Rignot and Kanagaratnam, 2006) were used together with SnowModel simulated SMB to estimate the average annual freshwater flux from the GrIS to the ocean for the period 1995 through 2007 (Table V). We recognize that ice sheets are highly dynamic and that the use of constant values for GrIS bottom melting and iceberg calving is a simple approximation. Zwally *et al.* (2002), Krabill *et al.* (2004); Rignot and Kanagaratnam (2006), and Rignot *et al.* (2008) suggest accelerated ice flow and enhanced iceberg calving associated with the observed thinning of the GrIS and the increasing supply of meltwater reaching the GrIS bed and lubricating the ice/bedrock interface. On the basis of our approximation, the average

Table V. Average annual freshwater flux from the GrIS to the Ocean for the period 1995 through 2007

Average annual freshwater flux (runoff and calving) from the GrIS to the Ocean from 1995 to 2007	GrIS runoff: supra- and subglacial contribution, km <sup>3</sup> y <sup>-1</sup> (%)		GrIS iceberg calving, km <sup>3</sup> y <sup>-1</sup> (%)	GrIS freshwater flux assessment, km <sup>3</sup> y <sup>-1</sup> (%)
	Supraglacial	Subglacial geothermal melt		
	397 (51%)	32 (4%) <sup>a</sup>	357 (45%) <sup>b</sup>	786 <sup>c</sup> 2.1 mm w.eq. y <sup>-1</sup>
		429 (55%)		

Freshwater flux is based on GrIS runoff (supra- and subglacial runoff) and GrIS iceberg calving.

<sup>a</sup> Values on geothermal contribution is estimated by Church *et al.* (2001).

<sup>b</sup> Values on GrIS iceberg calving is estimated by Rignot and Kanagaratnam (2006).

<sup>c</sup> The value is given in mm w.eq. y<sup>-1</sup> due to global eustatic sea level rise.

Table VI. Average annual GrIS net volume mass-balance change for the period 1995 through 2007

Average annual net mass loss (runoff and calving) from the GrIS to the Ocean from 1995 to 2007	Net GrIS loss: supra- and subglacial contribution, km <sup>3</sup> y <sup>-1</sup>		GrIS iceberg calving, km <sup>3</sup> y <sup>-1</sup>	Net GrIS Volume mass-balance change assessment, km <sup>3</sup> y <sup>-1</sup>
	Supraglacial	Subglacial geothermal melt		
	124	-32 <sup>a</sup>	-357 <sup>b</sup>	-265 <sup>c</sup> 0.7 mm w.eq. y <sup>-1</sup>
		92		

The net mass-balance change is based on changes in runoff (supra- and subglacial runoff) and iceberg calving.

<sup>a</sup> Values on geothermal contribution is estimated by Church *et al.* (2001).

<sup>b</sup> Values on GrIS iceberg calving is estimated by Rignot and Kanagaratnam (2006).

<sup>c</sup> The value is given in mm w.eq. y<sup>-1</sup> due to global eustatic net sea level rise.

annual GrIS net volume mass-balance is characterized by negative values (loss of mass) from 1995 through 2007, averaging  $-265 \text{ km}^3 \text{ y}^{-1}$  (Table VI). Observations by laser altimeter and Gravity Recovery and Climate Experiment (GRACE) of the GrIS confirm that the ice sheet is losing mass (Velicogna and Wahr, 2005; Chen *et al.*, 2006; Luthcke *et al.*, 2006; Thomas *et al.*, 2006). However, recognition of this trend is not unanimous (Johannessen *et al.*, 2005; Zwally *et al.*, 2005; Fettweis, 2007).

This study suggests an average annual (1995–2007) freshwater flux of approximately  $786 \text{ km}^3 \text{ y}^{-1}$  from the GrIS to the ocean (Table V). This flux has some uncertainties due to previously discussed SnowModel limitations and the use of average estimated values for geothermal melt and iceberg calving. The average GrIS freshwater runoff (supra- and subglacial) is approximately  $429 \text{ km}^3 \text{ y}^{-1}$  (~55% of total GrIS freshwater flux), where  $397 \text{ km}^3 \text{ y}^{-1}$  originates from the GrIS SMB runoff and  $32 \text{ km}^3 \text{ y}^{-1}$  is derived from subglacial geothermal bottom melting (Church *et al.*, 2001). The average contribution from GrIS iceberg calving is  $357 \text{ km}^3 \text{ y}^{-1}$  (Rignot and Kanagaratnam, 2006), which is ~45% of the total freshwater flux. A similar allocation was presented by Reeh *et al.* (1999) and Zwally and Giovinetto (2001), where surface melt water

runoff represents about half of the annual mass loss from the GrIS; iceberg calving and subglacial melting generates for the other half. Serreze *et al.* (2006) reported values of freshwater export from the Arctic Ocean to the Greenland Sea of  $4700 \text{ km}^3 \text{ y}^{-1}$ , with  $2300 \text{ km}^3 \text{ y}^{-1}$  as sea ice and  $2400 \text{ km}^3 \text{ y}^{-1}$  as upper-ocean freshwater. Therefore, the GrIS estimated freshwater flux of  $786 \text{ km}^3 \text{ y}^{-1}$  contributes approximately 17% of the total freshwater input to the Greenland Sea.

In the light of the global eustatic sea level rise, the total average annual GrIS freshwater flux contribution is around  $2.1 \pm 0.2 \text{ mm w.eq. y}^{-1}$ , indicating a 1995–2007 cumulative increase of ~28 mm w.eq. Further, the average GrIS net volume mass loss of  $265 (\pm 83) \text{ km}^3 \text{ y}^{-1}$  equals a total annual net eustatic sea level rise of  $0.7 \pm 0.2 \text{ mm w.eq. y}^{-1}$ , and a 1995–2007 cumulative increase of ~10 mm w.eq. This does not consider ocean water loss through evaporation or contribution by thermal expansion. According to Bindoff *et al.* (2007), GrIS contribution to the global sea level rise is  $0.05 \pm 0.12 \text{ mm w.eq. y}^{-1}$  during 1961 through 2003, and  $0.21 \pm 0.07 \text{ mm w.eq. y}^{-1}$  from 1993 to 2003, which is approximately three times lower than our estimate.

## SUMMARY AND CONCLUSION

Limited spatial measurements of key climate-hydrological-system components are a serious impediment to hydrological research efforts on the GrIS. This is especially important because freshwater runoff from the GrIS to the North Atlantic Ocean plays an important role in influencing global thermohaline circulation, salinity, sea-ice dynamics, and the global eustatic sea level rise. Thus, there is a clear need to explore modelling approaches that overcome chronic issues associated with data sparseness, lack of observations, and reliable future predictions. Such capabilities are useful for understanding how the GrIS responds to the changing climate.

This research has quantified GrIS water balance components, including the runoff flux to the ocean from 1995 through 2007, with focus on the year 2007 (record melt extent). A robust physically based state-of-the-art snow-evolution modelling system (SnowModel), modified for glacier-ice melt, was used. Owing to missing glacio-hydro-dynamic model routines, values from previous studies of GrIS geothermal melting and iceberg calving were adapted to provide corrected estimates of present water balance conditions.

There is a high degree of agreement between these GrIS simulations and recorded observations. Both indicate an increased surface melt extent and runoff, and a reduction in SMB during 1995–2007. Simulated values for the GrIS SMB, including runoff, are consistent with previous modelling studies. The GrIS freshwater flux (SMB, geothermal melting, and iceberg calving) has likely been a factor in global sea-level rise, contributing around 2.1 mm w.eq.  $y^{-1}$ , and cumulative around 28 mm w.eq. for the period to eustatic sea level rise. The average GrIS net loss equals a net eustatic sea level rise of 0.7 mm w.eq.  $y^{-1}$  and a cumulative increase of 10 mm w.eq. from 1995 through 2007 (not considering ocean loss by evaporation or contribution by thermal expansion).

Understanding the GrIS freshwater flux to the ocean is far from complete. How does the increasing volume of surface melt water, due to increasing melt content, affect the GrIS dynamics, the subglacier sliding processes, and the iceberg calving now and in a broader picture of global change? Further, how might GrIS runoff affect the global thermohaline circulation, salinity, and sea-ice dynamics at broader scales? These formidable questions promise to be at the frontier of Arctic and climate-change science investigations in the coming years.

## ACKNOWLEDGEMENTS

Thanks to the Cooperative Institute for Research in Environmental Science (CIRES), University of Colorado at Boulder, for hosting the first author from November 2007 to February 2008, and for providing satellite images and meteorological data for this study, and to the Faculty of Science and Institute of Low Temperature Science, Hokkaido University, Japan, for hosting the first author

from April through July 2008. Further thanks to the Danish Meteorological Institute (DMI), for providing WMO meteorological data. A special thanks to Dr Theodore Scambos, CIRES, University of Colorado at Boulder, for providing the Greenland digital elevation model. This work was supported by grants from the University of Alaska Presidential IPY Postdoctoral Foundation, the University of Alaska Fairbanks (UAF) Office of the Vice Chancellor for Research, and the FreshNor project by the Nordic Council of Ministers' Arctic Co-operation Programme. This study was carried out during the first author's IPY Presidential Post Doc. program at the UAF.

## REFERENCES

- Abdalati W, Steffen K. 1997. Snowmelt on the Greenland Ice sheet as derived from passive microwave satellite data. *Journal of Climate* **10**: 165–175.
- ACIA. 2005. *Arctic Climate Impact Assessment*. Cambridge University Press: New York; 1042.
- Allerup P, Madsen H, Vejen F. 1998. Estimating true precipitation in arctic areas. In *Proceedings Nordic Hydrological Conference*, Helsinki, Finland, Nordic Hydrological Programme Rep. 44, 1–9.
- Allerup P, Madsen H, Vejen F. 2000. Correction of precipitation based on off-site weather information. *Atmospheric Research* **53**: 231–250.
- Anderson EA. 1976. A point energy balance model of a snow cover. NOAA Technical Report NWS 19, NOAA: WASHINGTON, DC; 150.
- Bales RC, Guo Q, Shen D, McConnell JR, Du G, Burkhart JF, Spikes VB, Hanna E, Cappelen J. 2009. Annual accumulation for Greenland updated using ice core data developed during 2000–2006 and analysis of daily coastal meteorological data. *Journal of Geophysical Research* **114**: D06116, DOI:10.1029/2008JD011208.
- Bales RC, McConnell JR, Mosley-Thompson E, Csatho B. 2001a. Accumulation over the Greenland Ice Sheet from historical and recent records. *Journal of Geophysical Research* **106**(D24): 33813–33826.
- Bales RC, McConnell JR, Mosley-Thompson E, Lamorey G. 2001b. Accumulation Map for the Greenland Ice Sheet: 1971–1990. *Geophysical Research Letters* **28**(15): 2967–2970.
- Bamber J, Ekholm S, Krabill W. 2001. A new, high-resolution digital elevation model of Greenland fully validated with airborne laser altimeter data. *Journal of Geophysical Research* **106**(B4): 6733–6746.
- Barnes SL. 1964. A technique for maximizing details in numerical weather map analysis. *Journal of Applied Meteorology* **3**: 396–409.
- Barnes SL. 1973. Mesoscale objective analysis using weighted timeseries observations. NOAA Technical Memorandum ERL NSSL-62, National Severe Storms Laboratory: Norman, OK, 60.
- Bindoff NL, Willebrand J, Artale V, Cazenave A, Gregory J, Gulev S, Hanawa K, Le Quéré C, Levitus S, Nojiri Y, Shum CK, Talley LD, Unnikrishnan A. 2007. Observations: Oceanic Climate Change and Sea Level. In *Climate Change 2007: The Physical Science Basis*, Contribution of Working Group I to the Fourth Assessment Report of the Intergovernmental Panel on Climate Change, Solomon S, Qin D, Manning M, Chen Z, Marquis M, Averyt KB, Tignor M, Miller HL (eds). Cambridge University Press: Cambridge, New York.
- Boggild CE, Warren SG, Brandt RE, Brown KJ. 2006. Effects of dust and black carbon on albedo of the Greenland ablation zone. Abstract: American Geophysical Union, Fall Meeting 2006, abstract #U22A-05.
- Born EW, Böcher J. 2001. *The ecology of Greenland. Nuuk*. Ministry of Environment and Natural Resources: Nuuk; 429.
- Box J, Bromwich DH. 2004. Greenland ice sheet surface mass balance 1991–2000: Application of Polar MM5 mesoscale model and in situ data. *Journal of Geophysical Research* **109**: D16105, DOI:10.1029/2003JD004451.
- Box JE, Bromwich DH, Vennhuis BA, Bai L-S, Stroeve JC, Rogers JC, Steffen K, Haren T, Wang S-H. 2006. Greenland ice sheet surface mass balance variability (1988–2004) from calibrated Polar MM5 output. *Journal of Climate* **19**: 2783–2800.
- Broecker WS, Denton GH. 1990. The role of ocean-atmosphere reorganization in glacial cycles. *Quaternary Science Reviews* **9**: 305–341.
- Broecker WS, Peteet DM, Rind D. 1985. Does the ocean-atmosphere system have more than one stable mode of operation. *Nature* **315**: 21–26.

- Brown RD, Brasnett B, Robinson D. 2003. Gridded North American monthly snow depth and snow water equivalent for GCM evaluation. *Atmosphere-Ocean* **41**: 1–14.
- Bruland O, Liston GE, Vonk J, Sand K, Killingtveit A. 2004. Modelling the snow distribution at two High-Arctic sites at Svalbard, Norway, and at a Sub-Arctic site in Central Norway. *Nordic Hydrology* **35**(3): 191–208.
- Chen JL, Wilson CR, Tapley BD. 2006. Satellite gravity measurements confirm accelerated melting of Greenland Ice Sheet. *Science* **313**: 1958–1960, DOI:10.1126/science.1129007.
- Church JA, Greory JM, Huybrechts P, Kuhn M, Lambeck C, Nhuan MT, Qin D, Woodworth PL. 2001. In *Change in Sea Level, in Climate change 2001: The Scientific Basis—Contribution of Working Group I to the Third Assessment Report of the Intergovernmental Panel on Climate Change*, Huoghton JT, Ding Y, Griggs DJ, Noguer M, van der Linden PJ, Xiaosu D. (eds). Cambridge University Press: New York: 639–694.
- Chylek P, Dubey MK, Lesins G. 2006. Greenland warming of 1920–1930 and 1995–2005. *Geophysical Research Letters* **33**: L11707, DOI:10.1029/2006GL026510, 2006.
- Dodson R, Marks D. 1997. Daily air temperature interpolation at high spatial resolution over a large mountainous region. *Climate Research* **8**: 1–20.
- Dowdeswell JA, Hagen JO, Björnsson H, Glazovsky AF, Harrison WD, Holmlund P, Jania J, Koerner RM, Lefauconnier B, Ommanney CSL, Thomas RH. 1997. The Mass balance of Circum-Arctic Glaciers and recent climate change. *Quaternary Research* **48**: 1–4, QR971900: 1–14.
- Fettweis X. 2007. Reconstruction of the 1979–2006 Greenland ice sheet surface mass balance using the regional climate model MAR. *Cryosphere* **1**: 21–40.
- Førland EJ, Hanssen-Bauer I. 2003. Climate variations and implications for precipitations types in the Norwegian Arctic. Report 24/02, Norwegian Meteorological Institute: 21.
- Greene EM, Liston GE, Pielke RA. 1999. Simulation of above treeline snowdrift formation using a numerical snowtransport model. *Cold Regions Science and Technology* **30**: 135–144.
- Hanna E, Box J, Huybrechts P. 2007. Greenland Ice Sheet mass balance. Arctic Report Card 2007, update to State of Arctic Report 2006, NOAA, Available online at <http://www.arctic.noaa.gov/reportcard/>.
- Hanna E, Cappelen J, Fettweis X, Huybrechts P, Luckman A, Ribergaard MH. 2009. Hydrologic response of the Greenland Ice sheet: the role of oceanographic warming. *Hydrological Processes* **23**(1): 7–30.
- Hanna E, Huybrechts P, Janssens I, Cappelen J, Steffen K, Stephens A. 2005. Runoff and mass balance of the Greenland ice sheet: 1958–2003. *Journal of Geophysical Research* **110**: 1–16.
- Hanna E, Huybrechts P, Mote T. 2002. Surface mass balance of the Greenland ice sheet from climate-analysis data and accumulation/runoff models. *Annals of Glaciology* **35**: 67–72.
- Hanna E, Huybrechts P, Steffen K, Cappelen J, Huff R, Shuman C, Irvine-Fynn T, Wise S, Griffiths M. 2008. Increased Runoff from melt from the Greenland Ice Sheet: A response to Global Warming. *Journal of Climate* **21**: 331–341.
- Hansen BU, Sigsgaard C, Hinkler J, Mernild SH, Petersen D, Rasch M, Tamstorf MP, Hasholt B, Rasmussen L, Cappelen J. 2008. Present day climate at Zackenberg. In *High-Arctic Ecosystem Dynamics in a Changing Climate: Ten Years of Monitoring and Research at Zackenberg Research Station, Northeast Greenland*, vol. 40, Meltofte H, Christensen TR, Elberling B, Forchhammer MC, Rasch M (eds). Hydrology and Transport of Sediment and Solutes at Zackenberg, Advances in Ecological Research: London; 197–221.
- Hasholt B, Bobrovitskaya N, Bogen J, McNamara J, Mernild SH, Milbourn D, Walling DE. 2006. Sediment transport to the Arctic Ocean and adjoining cold oceans. *Nordic Hydrology* **37**(4–5): 413–432.
- Hasholt B, Liston GE, Knudsen NT. 2003. Snow distribution modelling in the Ammassalik region, southeast Greenland. *Nordic Hydrology* **34**: 1–16.
- Hasholt B, Mernild SH. 2006. Glacial erosion and sediment transport in the Mittivakkat Glacier catchment, Ammassalik Island, Southeast Greenland, 2005. Sediment Dynamics and the Hydeomorphology of Fluvial Syatems (Proceedings of a symposium held in Dundee, UK, July 2006). IAHS Publication 306, 45–55.
- Hasholt B, Mernild SH. 2008. Hydrology, sediment transport, and water resources of Ammassalik Island, SE Greenland. *Danish Journal of Geography* **108**(1): 75–97.
- Hiemstra CA, Liston GE, Reiners WA. 2002. Snow Redistribution by Wind and Interactions with Vegetation at Upper Treeline in the Medicine Bow Mountains, Wyoming. *Arctic Antarctic and Alpine Research* **34**: 262–273.
- Hiemstra CA, Liston GE, Reiners WA. 2006. Observing, modelling, and validating snow redistribution by wind in a Wyoming upper treeline landscape. *Ecological Modelling* **197**: 35–51.
- Hinzman LD, Bettez ND, Bolton WB, Chapin FS, Dyrugerov MB, Fastie CL, Griffith B, Hollister RD, Hope A, Huntington HP, Jensen AM, Jia GJ, Joergensen T, Kane DL, Klein DR, Kofinas G, Lynch AH, Lloyd AH, McGuire AD, Nelson FE, Oechel WC, Osterkamp TE, Racine CH, Romanovsky VE, Stone RS, Stow DA, Sturm M, Tweedie CE, Vourlitis GL, Walker MD, Walker DA, Webber PJ, Welker JM, Winker KS, Yoshikawa K. 2005. Evidence and implications of recent climate change in Northern Alaska and other Arctic regions. *Climatic Change* **72**: 251–298.
- IPCC. 2007. Summary for poicymakers. In *Climate Change 2007: The Physical Science Basis*, Contribution of Working Group I to the Fourth Assessment Report of the Intergovernmental Panel on Climate Change, Solomon S, Qin D, Manning M, Chen Z, Marquis M, Averyt KB, Tignor M, Miller HL (eds). Cambridge University Press: Cambridge, New York.
- Iziomon MG, Mayer H, Matzarakis A. 2003. Downward atmospheric longwave irradiance under clear and cloudy skies: Measurement and parameterization. *Journal of Atmospheric and Solar-Terrestrial Physics* **65**: 1107–1116.
- Janssens I, Huybrechts P. 2000. The treatment of meltwater retention in Mass-balance parameterisation of the Greenland Ice Sheet. *Annals of Glaciology* **31**: 133–140.
- Johannessen OM, Khvorostovsky K, Miles MW, Bobylev LP. 2005. Recent ice sheet growth in the interior of Greenland. *Scienceexpress*: 1013–1016, DOI:10.1126/science.1115356.
- Koch SE, DesJardins M, Kocin PJ. 1983. An interactive Barnes objective map analysis scheme for use with satellite and conventional data. *Journal of Climate and Applied Meteorology* **22**: 1487–1503.
- Krabill W, Hanna E, Huybrechts P, Abdalati W, Cappelen J, Csatho B, Frederick E, Manizade S, Martin C, Sonntag J, Swift R, Thomas R, Yungel J. 2004. Greenland ice sheet: Increased coastal thinning. *Geophysical Research Letters* **31**: L24402, DOI:10.1029/2004GL021533.
- Kunkel KE. 1989. Simple procedures for extrapolation of humidity variables in the mountains western United States. *Journal of Climate* **2**: 656–669.
- Liston GE. 1995. Local Advection of Momentum, Heat, and Moisture during the Melt of Patchy Snow Covers. *Journal of Applied Meteorology* **34**(7): 1705–1715.
- Liston GE. 2004. Representing subgrid snow cover heterogeneities in regional and global models. *Journal of Climate* **17**: 1381–1397.
- Liston GE, Elder K. 2006a. A distributed snow-evolution modeling system (SnowModel). *Journal of Hydrometeorology* **7**: 1259–1276.
- Liston GE, Elder K. 2006b. A meteorological distribution system for high resolution terrestrial modeling (MicroMet). *Journal of Hydrometeorology* **7**: 217–234.
- Liston GE, Hall DK. 1995. An energy-balance model of lake-ice evolution. *Journal of Glaciology* **41**: 373–382.
- Liston GE, Haehnel RB, Sturm M, Hiemstra CA, Berezovskaya S, Tabler RD. 2007. Simulating complex snow distributions in windy environments using SnowTran-3D. *Journal of Glaciology* **53**: 241–256.
- Liston GE, McFadden JP, Sturm M, Pielke RA Sr. 2002. Modeled changes in arctic tundra snow, energy, and moisture fluxes due to increased shrubs. *Global Change Biology* **8**: 17–32.
- Liston GE, Sturm M. 1998. A snow-transport model for complex terrain. *Journal of Glaciology* **44**: 498–516.
- Liston GE, Sturm M. 2002. Winter precipitation patterns in Arctic Alaska determined from a Blowing-Snow Model and Snow-Depth observations. *Journal of Hydrometeorology* **3**: 646–659.
- Liston GE, Sturm M. 2004. The role of winter sublimation in the Arctic moisture budget. *Nordic Hydrology* **35**(4): 325–334.
- Liston GE, Winther J-G. 2005. Antarctic surface and subsurface snow and ice melt fluxes. *Journal of Climate* **18**(10): 1469–1481.
- Liston GE, Winther J-G, Bruland O, Elvehøy H, Sand K. 1999. Belowsurface ice melt on the coastal Antarctic ice sheet. *Journal of Glaciology* **45**(150): 273–285.
- Liston GE, Winther J-G, Bruland O, Elvehøy H, Sand K, Karlöf L. 2000. Snow and blue-ice distribution patterns on the coastal Antarctic ice sheet. *Antarctic Science* **12**(1): 69–79.
- Luthcke SB, Zwally HJ, Abdalati W, Rowlands DD, Ray RD, Nerem RS, Lemoine FG, McCarthy JJ, Chinn DS. 2006. Recent Greenland Ice Mass Loss by drainage system from satellite gravity observations. *Science* **314**(5803): 1286, DOI:10.1126/science.1130776.
- McConnell JR, Lamorey G, Hanna E, Mosley-Thompson E, Bales RC, Belle-Oudry D, Kyne JD. 2001. Annual new snow accumulation over

- southern Greenland from 1975 to 1998. *Journal of Geophysical Research* **106**(D24): 33827–33838.
- Mernild SH, Hasholt B. 2006. Climatic control on river discharge simulations from the Mittivakkat Glacier catchment, Ammassalik Island, SE Greenland. *Nordic Hydrology* **37**(4–5): 327–346.
- Mernild SH, Liston GE. 2009. The influence of air temperature inversion on snow melt and glacier surface mass-balance simulations, SW Ammassalik Island, SE Greenland. In review *Journal of Applied Meteorology and Climate*.
- Mernild SH, Liston GE, Hasholt B. 2007. Snow-Distribution and Melt Modeling for Glaciers in Zackenberg River Drainage Basin, NE Greenland. *Hydrological Processes* **21**: 3249–3263, DOI: 10.1002/hyp.6500.
- Mernild SH, Hasholt B, Liston GE. 2006a. Water flow through Mittivakkat Glacier, Ammassalik Island, SE Greenland. *Danish Journal of Geography* **106**(1): 25–43.
- Mernild SH, Liston GE, Hasholt B, Knudsen NT. 2006b. Snow-Distribution and melt Modeling for Mittivakkat Glacier, Ammassalik Island, SE Greenland. *Journal of Hydrometeorology* **7**: 808–824.
- Mernild SH, Liston GE, Hiemstra CA, Steffen K. 2009. Record 2007 Greenland Ice Sheet surface melt-extent and runoff. *EOS, Transactions-American Geophysical Union* **90**(2): 13–14.
- Mernild SH, Liston GE, Hiemstra CA, Steffen K. 2008a. Surface Melt Area and Water Balance Modeling on the Greenland Ice Sheet 1995–2005. *Journal of Hydrometeorology* **9**(6): 1191–1211, DOI: 10.1175/2008JHM957.1.
- Mernild SH, Liston GE, Hasholt B. 2008b. East Greenland freshwater runoff to the Greenland-Iceland-Norwegian Seas 1999–2004 and 2071–2100. *Hydrological Processes* **22**: 4571–4586, DOI: 10.1002/hyp.7061.
- Mernild SH, Kane DL, Hansen BU, Jakobsen BH, Hasholt B, Knudsen NT. 2008c. Climate, glacier mass balance, and runoff (1993–2005) Mittivakkat Glacier catchment, Ammassalik Island, SE Greenland, and in a long term perspective (1898–1993). *Hydrology Research* **39**(4): 239–256.
- Mernild SH, Hasholt B, Liston GE. 2008d. Climatic control on river discharge simulations, Zackenberg River Drainage basin, NE Greenland. *Hydrological Processes* **22**: 1932–1948, DOI: 10.1002/hyp.6777.
- Mernild SH, Liston GE, Kane DL, Knudsen NT, Hasholt B. 2008e. Snow, runoff, and mass balance modeling for entire Mittivakkat Glacier (1998–2006), Ammassalik Island, SE Greenland. *Danish Journal of Geography* **108**(1): 121–136.
- Moritz RE, Bitz CM, Steig EJ. 2002. Dynamics of recent climate change in the Arctic. *Science* **297**: 1497–1502.
- Mote TL. 2003. Estimations of runoff rates, mass balance, and elevation changes on Greenland ice sheet from passive microwave observations. *Journal of Geophysical Research* **108**(D2): 4052.
- Mote TL. 2007. Greenland surface melt trends 1973–2007: Evidence of a large increase in 2007. *Geophysical Research Letters* **34**: L22507, DOI:10.1029/2007GL031976.
- Nakicenovic N, Alcamo J, Davis G, de Vries B, Fenhann J, Ga Yn S, Gregory K, Grübler A, Jung TY, Kram T, La Rovere EL, Michaelis L, Mori S, Morita T, Pepper W, Pitcher H, Price L, Riahi K, Roehrl A, Rogner H-H, Sankovski A, Schlesinger M, Shukla P, Smith S, Swart R, van Rooijen S, Victor N, Dadi Z. 2000. *IPCC Special Report on Emissions Scenarios*. Cambridge University Press: Cambridge.
- Pielke RA Sr. 2002. *Mesoscale Meteorological Modeling*. Academic Press; 676.
- Pomeroy JW, Brun E. 2001. Physical properties of snow. In *Snow Ecology: An Interdisciplinary Examination of Snow-covered Ecosystems*, Jones HG, Pomeroy JW, Walker DA, Hoham RW (eds). Cambridge University Press: Cambridge; 45–118.
- Prasad R, Tarboton DG, Liston GE, Luce CH, Seyfried MS. 2001. Testing a blowing snow model against distributed snow measurements at Upper Sheep Creek. *Water Resources Research* **37**: 1341–1357.
- Reeh N, Mayer C, Miller H, Thomson HH, Weidick A. 1999. Present and past climate control on fjord glaciations in Greenland: Implications for IRD-deposition in the sea. *Geophysical Research Letters* **26**: 1039–1042.
- Rignot E, Box JE, Burgess JEE, Hanna E. 2008. Mass balance of the Greenland ice Sheet from 1958 to 2007. *Geophysical Research Letters* **35**: L20502, DOI:10.1029/2008GL035417.
- Rignot E, Kanagaratnam P. 2006. Changes in the Velocity Structure of the Greenland Ice Sheet. *Science* **315**: 1559–1561.
- Ryan BC. 1977. A mathematical model for diagnosis and prediction of surface winds in mountains terrain. *Journal of Applied Meteorology* **16**: 1547–1564.
- Rysgaard S, Vang T, Stjernholm M, Rasmussen B, Windelin A, Kiilsholm S. 2003. Physical conditions, carbon transport, and climate change impacts in a Northeast Greenland Fjord. *Arctic Antarctic and Alpine Research* **35**: 301–312.
- Scambos T, Haran T. 2002. An image-enhanced DEM of the Greenland Ice Sheet. *Annals of Glaciology* **34**: 291–298.
- Serreze MC, Baret AP, Slater AG, Woodgate RA, Aagaard K, Lammers RB, Steele M, Moritz R, Meredith M, Lee CM. 2006. The large-scale freshwater cycle of the Arctic. *Journal of Geophysical Research* **111**: C11010, DOI: 10.1029/2005JC003424.
- Serreze MC, Barry RG. 2005. *The Arctic Climate System*, Cambridge University Press: Cambridge; 385 pp.
- Serreze MC, Walsh JE, Chapin FS III, Osterkamp M, Dyrugerov M, Romanovsky V, Oechel WC, Morison J, Zhang T, Barry RG. 2000. Observational evidence of recent change in the northern high-latitude environment. *Climatic Change* **46**: 159–207.
- Sturm M, Holmgren J, Liston GE. 1995. Seasonal snow cover classification system for local to global applications. *Journal of Climate* **8**: 1261–1283.
- Su F, Adam JC, Trenberth KE, Lettenmaier DP. 2006. Evaluation of surface water fluxes of the pan-Arctic land region with a land surface model and ERA-40 reanalysis. *Journal of Geophysical Research* **111**: D05110, DOI: 10.1029/2005JD006387.
- Tedesco M. 2007. A new record in 2007 for melting in Greenland. *EOS* **88**(39): 383.
- Thomas R, Frederick E, Krabill W, Manizade S, Martin C. 2006. Progressive increase in ice loss from Greenland. *Geophysical Research Letters* **33**: L10503, DOI:10.1029/2006GL026075.
- Thornton PE, Running SW, White MA. 1997. Generating surfaces of daily meteorological variables over large regions of complex terrain. *Journal of Hydrology* **190**: 214–251.
- Velicogna I, Wahr J. 2005. Greenland mass balance from GRACE. *Geophysical Research Letters* **32**: L18505, DOI:10.1029/2005GL023955.
- Vorosmarty CJ, Hinzman LD, Peterson BJ, Bromwich DH, Hamilton LC, Morison J, Romanovsky VE, Sturm M, Webb RS. 2001. The hydrological cycle and its role in Arctic and global environmental change: A reitional and strategy for synthesis study, 84, Arct. Res. Consortium of the U.S., Fairbanks, Alaska.
- Walcek CJ. 1994. Cloud cover and its relationship to relative humidity during a spring midlatitude cyclone. *Monthly Weather Review* **122**: 1021–1035.
- Yang D, Ishida S, Goodison BE, Gunther T. 1999. Bias correction of precipitation data for Greenland. *Journal of Geophysical Research-Atmospheres* **104**(D6): 6171–6181.
- Zwally JH, Abdalati W, Herring T, Larson K, Saba J, Steffen K. 2002. Surface melt-induced acceleration of Greenland ice-sheet flow. *Science* **297**: 218–222.
- Zwally JH, Giovinetto MB. 2001. Balance mass flux and ice velocity across the equilibrium line in drainage systems of Greenland. *Journal of Geophysical Research* **106**(33): 717–728.
- Zwally JH, Giovinetto M, Li J, Cornejo H, Beckley M, Brenner A, Saba J, Yi D. 2005. Mass changes of the Greenland and Antarctic ice sheets and shelves and contributions to sea-level rise: 1992–2002. *Journal of Glaciology* **51**(175): 509–527(19).